We are IntechOpen,
the world's leading publisher of
Open Access books
Built by scientists, for scientists

6,900
Open access books available

186,000
International authors and editors

200M
Downloads

Our authors are among the

154
Countries delivered to

TOP 1%
most cited scientists

12.2%
Contributors from top 500 universities

CLARIVATE ANALYTICS
BOOK CITATION INDEX
INDEXED

WEB OF SCIENCE™

Selection of our books indexed in the Book Citation Index
in Web of Science™ Core Collection (BKCI)

Interested in publishing with us?
Contact book.department@intechopen.com

Numbers displayed above are based on latest data collected.
For more information visit www.intechopen.com

Calibration of Measuring Systems Based on Maximum Dynamic Error

Krzysztof Tomczyk
Cracow University of Technology, Faculty of Electrical and Computer Engineering,
Poland

1. Introduction

This chapter presents methods and algorithms for determining the maximum errors which can be generated by measuring systems in reference to their standards. The application of such errors in the process of calibration of measuring systems intended for measurement of dynamic signals is discussed in detail. The problem of maximum errors lies in the fact that it is impossible to analyze the full range of all possible dynamic input signals. Therefore we find out the one that represents all signals. It is the signal generating errors of maximum value.

The existence and availability of signals maximizing both the integral-square error and the absolute value of error are discussed, and relevant solutions are presented. Moreover, the constraints imposed on the input signal are analyzed. These constraints refer to the magnitude as well as maximum rate of signal change. The latter constraint is applied in order to match the dynamic properties of the signal to the dynamic properties of the system under test.

In the relevant literature it was proved that the signals maximizing the errors in question always achieve one of the constraints imposed on it. If only the signal amplitude is constrained, the maximizing signal is always of the 'bang-bang' type, while in the case of two constraints relating to the magnitude and the rate of change such a signal can be only of triangular or trapezoid shape with slopes resulting from the values of constraints.

For the integral-square error, no analytic solution referring to the shape of the maximizing signal has been found so far. This is why the solution of this problem presented in the chapter is based on the application of the genetic algorithm method. This method guarantees that the results are obtained in minimized calculation time which depends only on the assumed number of population, the value of the stop condition and number of assumed switches.

In the case of the absolute error, the analytical formulae and algorithm which give precise results and can be realized in a very short calculation time are considered. The signal maximizing this criterion is presented in the form of figures showing the successive steps of proceeding as well as the error shape corresponding to this signal.

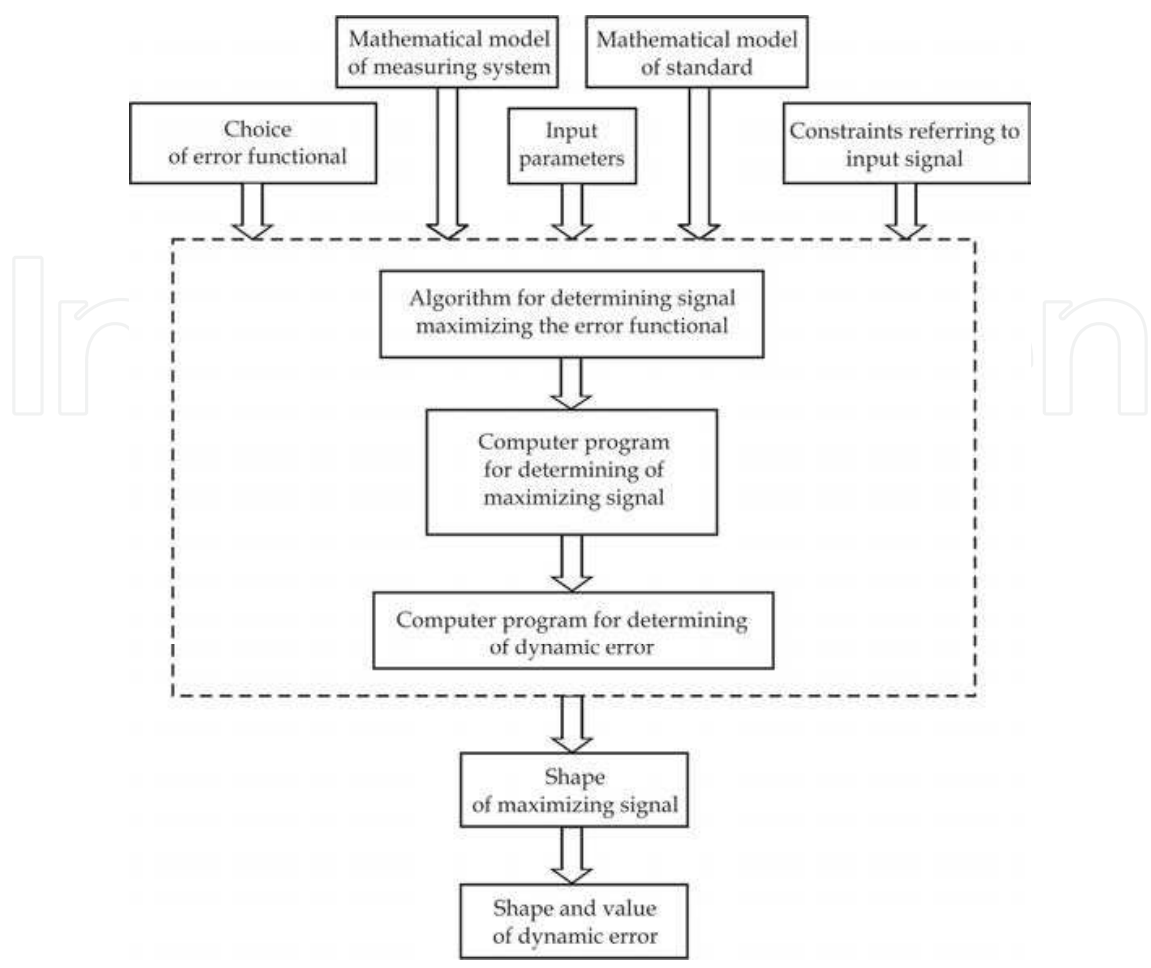Fig. 1 presents a block diagram of our calibration process.

Fig. 1. Block diagram of calibration process of measuring systems based on maximum dynamic error.

In this chapter respective procedures and essential mathematical operations, which allow carrying out the calibration process according to the block diagram presented above, are discussed in detail. In part two the input-output relations of measuring systems are discussed, part three is devoted to the synthesis of the mathematical model of standard and, in part four error functionals are presented and analyzed. The problem of existence and attainability of maximizing signals is discussed in part five, while parts six and seven present the procedures for determining signals maximizing the integral-square error and the absolute value of error.

The optimization of the *minimax* type on the basis of maximizing signals is presented in part eight. Such optimization is performed in two steps. In the first step the input signal maximizing the assumed error functional is determined, while in the second step the model parameters optimization based on the obtained signal is performed.

The identification problem of the mathematical model of measuring system is omitted in this chapter as it does not concern the theory of calibration. It was assumed that this model exist and is given in the form of transfer function.

The practical application of the presented theory and algorithms is illustrated on the example of low-pass measuring systems.

2. Input-output relations of measuring systems

Let output signal $y(t)$ of calibrated system be described by integral convolution

$$y(t) = \int_0^t x(\tau)h(t-\tau)d\tau, \ t \in [0, T]$$
$$h(t) = h_m(t) - h_s(t)$$

(1)

where: $x(t)$ - input signal, $h_m(t)$, $h_s(t)$ - impulse responses of system and its standard.

The convolution (1) can be presented in a discrete form as a sum

$$y(n) = \Delta \sum_{k=0}^n x(k)h(n-k), \ n = 0,1,...,N-1$$

(2)

$$\Delta - \text{ sample interval of } T$$

or in matrix form

$$\begin{bmatrix} y_0 \\ y_1 \\ y_2 \\ ... \\ y_{N-1} \end{bmatrix} = \Delta \begin{bmatrix} h_0 & 0 & 0 & ... & 0 \\ h_1 & h_0 & 0 & ... & 0 \\ h_2 & h_1 & h_0 & ... & 0 \\ ... & ... & ... & ... & ... \\ h_{N-1} & h_{N-2} & h_{N-3} & ... & h_0 \end{bmatrix} \begin{bmatrix} x_0 \\ x_1 \\ x_2 \\ ... \\ x_{N-1} \end{bmatrix}$$

(3)

In many cases it is convenient to present the output $y(t)$ by means of the following formula

$$y(n) = \frac{1}{n+1} \sum_{m=0}^n \left[\sum_{k=0}^n x(k)e^{-i\frac{2\pi}{n+1}mk} \sum_{k=0}^n h(k)e^{-i\frac{2\pi}{n+1}mk} \right] e^{i\frac{2\pi}{n+1}mn} \Delta$$

(4)

or by the Fourier transform

$$Y(i\omega) = X(i\omega)H(i\omega)$$
$$Y(i\omega) = F\{y(n)\}, \ X(i\omega) = F\{x(n)\}, \ H(i\omega) = F\{h(n)\}$$

(5)

where F presents the DFT or FFT (Tomczyk, 2011).

Multiplication of the Fourier transformations in (5) gives

$$\text{Re } Y(i\omega) = \text{Re } X(i\omega)\text{Re } H(i\omega) - \text{Im } X(i\omega)\text{Im } H(i\omega)$$
$$\text{Im } Y(i\omega) = \text{Im } X(i\omega)\text{Re } H(i\omega) + \text{Re } X(i\omega)\text{Im } H(i\omega)$$

(6)

From Eq. (6) we get

$$y(n) = IF[\text{Re } Y(i\omega) + j\text{Im } Y(i\omega)]\Delta$$

(7)

where IF denotes inverse DFT.

In state space we have

$$y(n + 1) = \mathbf{\Phi} y(n) + \mathbf{\Psi} x(n)$$

$$y(\cdot) - \text{ state vector}, y(\cdot) \in \Re^p, p - \text{ number of state variables} \qquad (8)$$

$$x(\cdot) - \text{ input (control) vector}, x(\cdot) \in \Re^p, q - \text{ number of inputs}$$

Presenting (8) in the matrix form, we have

$$\begin{bmatrix} y(n+1) \\ \vdots \\ y_p(n+1) \end{bmatrix} = \begin{bmatrix} \varphi_{1,1} & \cdots & \varphi_{1,p} \\ \vdots & & \vdots \\ \varphi_{p,1} & \cdots & \varphi_{p,p} \end{bmatrix} \begin{bmatrix} y(n) \\ \vdots \\ y_p(n) \end{bmatrix} + \begin{bmatrix} \psi_1 \\ \vdots \\ \psi_p \end{bmatrix} x(n) \qquad (9)$$

where

$$\mathbf{\Phi}_{(pxp)} = e^{\mathbf{A}\Delta}$$

$$\mathbf{A}_{(pxp)} - \text{state matrix} \qquad (10)$$

and

$$\mathbf{\Psi}_{(pxq)} = \int_0^\Delta e^{\mathbf{A}t} dt \, \mathbf{B} = \mathbf{A}^{-1}(e^{\mathbf{A}\Delta} - \mathbf{I})\mathbf{B} \qquad (11)$$

$$\mathbf{B}_{(pxq)} - \text{ input (control) matrix}, \mathbf{I}_{(pxp)} - \text{unit matrix}$$

3. Synthesis of mathematical model of standard

The calibration procedures for measuring systems intended for measurement of static quantities are commonly known and have been used for a long time in measuring practice. They cover the hierarchy of standards and calibrations circuits.

For measuring systems intended for measurement of dynamic quantities neither legal regulations concerning hierarchy of their accuracy nor specific calibrating procedures have been worked out so far. It results from the fact that for such systems input signals are time dependent, often undetermined, and whose shapes cannot be predicted in advance. The second reason is that the problem of standards for such systems has not been solved till now, because various measuring systems fulfill different objective functions (Tomczyk&Sieja, 2006). For such a situation we expect that models of standard will satisfy mathematical notation of these functions. In the dynamic measurement selection of standard parameters can be realized by means of optimization methods, which assure the conditions of non-distortion transformation, or by means of ideal filters of a band-pass which corresponds to the range of the work of the calibrated system. For low-pass systems this standard is given by

$$H_s(i\omega) = \begin{cases} c \cdot e^{-st_0} & \text{for } 0 \le \omega \le \omega_m \\ 0 & \text{for } \omega \ge \omega_m \end{cases} \qquad (12)$$

Impulse response of (12) equals

$$h_s(t) = \frac{c}{\pi} \omega_m Sa\left[\omega_m\left(t - t_0\right)\right] \tag{13}$$

where: c - amplification coefficient, t_0 - filter delay, ω_m - cut-off frequency.

4. Error functionals

Dynamic errors applied in our calibration are defined in different function spaces by means of chosen functionals. If the values of these functionals are determined by means of maximizing signals, it means that they will be valid for any dynamic signals which can appear at the input of the calibrated system. In this way all the possible input signals are included in this special, maximizing one.

The process of maximum error determination requires a special input signal to be used, which warrants that the error determined with it will always be higher or at least equal to the value generated by any other signal. The solution of this problem needs to prove that there exists a signal maximizing the chosen error functional at all, and if so, to elaborate a suitable procedure for its determination. The maximum values of error can constitute the base to work out the hierarchy of accuracy for instruments for dynamic measurement.

The integral-square error

$$I(x) = \int_0^T y^2(t)\,dt \tag{14}$$

and absolute value of error

$$D(x) = |y(t)| \tag{15}$$

will be discussed as an example.

The choice of the functionals (14) and (15) results from the fact that they are the most common in many different engineering domains.

5. Existence and attainability of maximizing signals

In (Layer, 2002, Layer&Tomczyk, 2010) it was proved that signals maximizing $I(x)$ and $D(x)$ functionals in $[0,T]$ always achieve one of the constraints imposed on them.

The constraints in question concern the magnitude a and rate of change ϑ. For systems described by means of linear differential equations, the constraint of magnitude $x(t)$ results from the measuring range of this system. Imposition on the signal of only this one constraint gives the solutions of 'bang-bang' type. As a result unexpected great values of errors are generated. It is affected by the dynamics of 'bang-bang' signals which have infinitely high derivative values in the instants of switching. Outside of these instants, they have constant values. Because of this, the 'bang-bang' signals are not matched to the dynamics of physically existing systems, since they can only transmit signals of a limited value of the rate of change. In order to match the dynamic behaviour of the input signals an additional constraint resulting from the dynamic properties of the calibrated system should be imposed. Proper matching is obtained by restricting the maximum rate of change ϑ of the signal.

5.1 Constraints of signal

In the case of two simultaneous constraints a and ϑ, the maximizing signal has a triangular shape with the slopes inclination $\pm \alpha$,

$$\vartheta = tg\alpha \tag{16}$$

or a trapezoid shape with the slopes inclination $\pm \alpha$ and the height a.

We can analyze here two different premises referring to the rate of change ϑ value. The first one refers to the time domain

$$\vartheta \leq \max_{t \in [0,T]} |\dot{x}(t)| \leq \max_{t \in [0,\infty]} |h(t)| \tag{17}$$

where $h(t)$ denotes the impulse responses of the system.

In the frequency domain constraint ϑ results from the maximum frequency of the band-pass of system ω_m. In this case we have

$$\vartheta \leq \max_{t \in [0,T]} |(a\sin \omega_m t)'| = a\omega_m. \tag{18}$$

where A denotes amplitude.

6. Procedure for determining signals maximizing the integral-square error

For the integral-square error (14) good results in the determining of signals maximizing this functional are achieved by the application of genetic algorithm. Fig. 2 presents a flowchart of this algorithm.

If $I_i(x) > I_h(x)$, the switch $s1$ takes the position 1 and the value of $I_i(x)$ is assigned to $I_h(x)$. Then $I_h(x)$ is stored in the buffer memory. Parallel to this operation, the vector of switching signal $x_i(t)$ and the output $y_i(t)$ are saved in the memory.

For $i = N$ the switch $s2$ changes the position from 0 to 1 and the values $x_i(t)$, $y_i(t)$ and $I_h(x)$ are assigned to $x_0(t)$, $y(t)$ and $I_{\max}(x)$, respectively.

The algorithm presented in Fig.3 includes three main operations: reproduction, crossing and mutation.

In the first step, the initial population $(c_{11}, c_{12}, ..., c_{1n})$ including an even number of chromosomes is selected at random. Each chromosome consists of detectors $(d_{11}, d_{12}, ..., d_{1m}), (d_{21}, d_{22}, ..., d_{2m}), ..., (d_{n1}, d_{n2}, ..., d_{nm})$, which correspond to the switching times of x_i signal. For each chromosome the error (14) is determined. Then on the basis of the obtained results, adaptation coefficient I_N is calculated as

$$I_N = I_{c_1} + I_{c_2} + .. + I_{c_n} \tag{19}$$

This coefficient presents the total error generated by all chromosomes (Tomczyk, 2006).
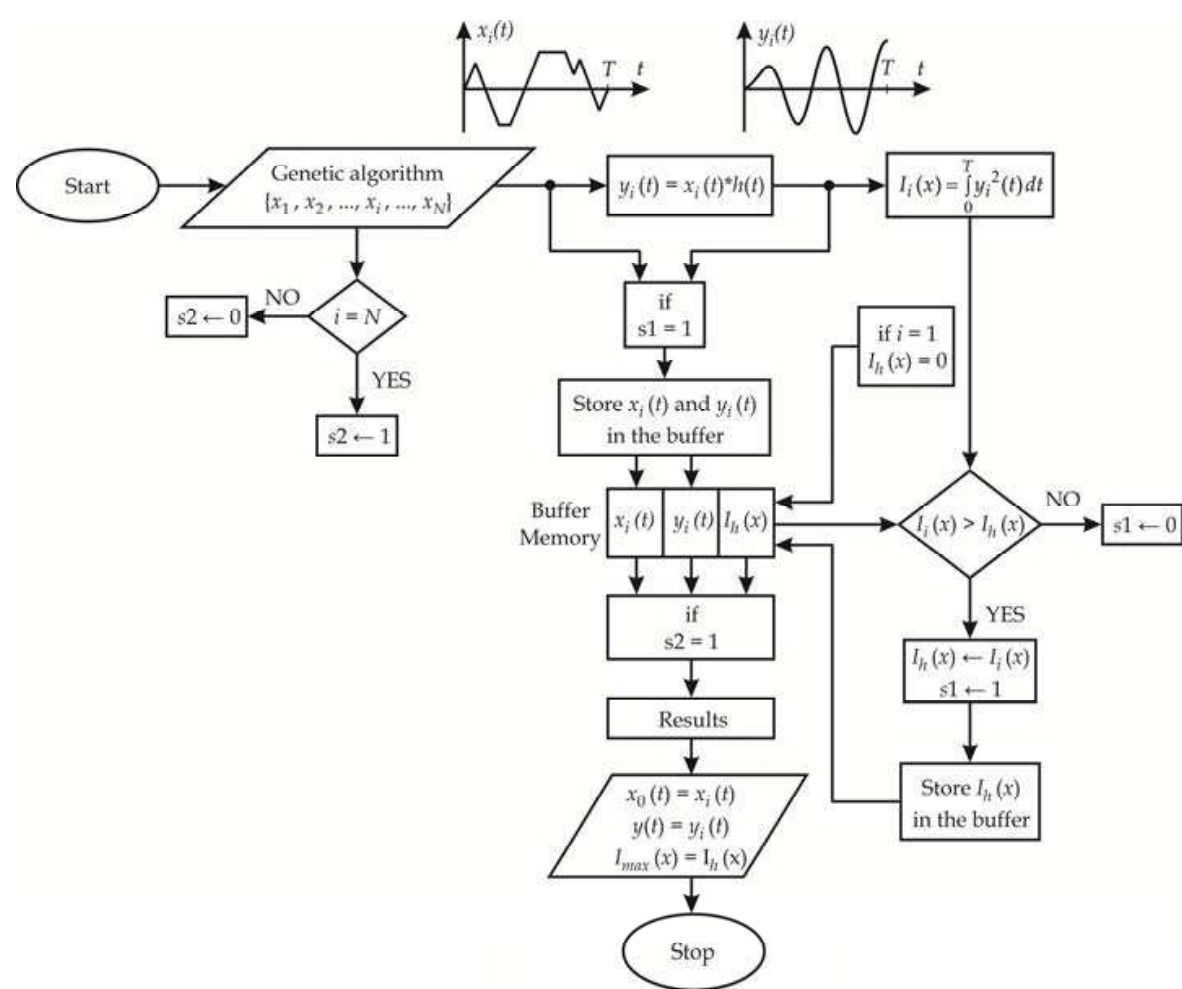
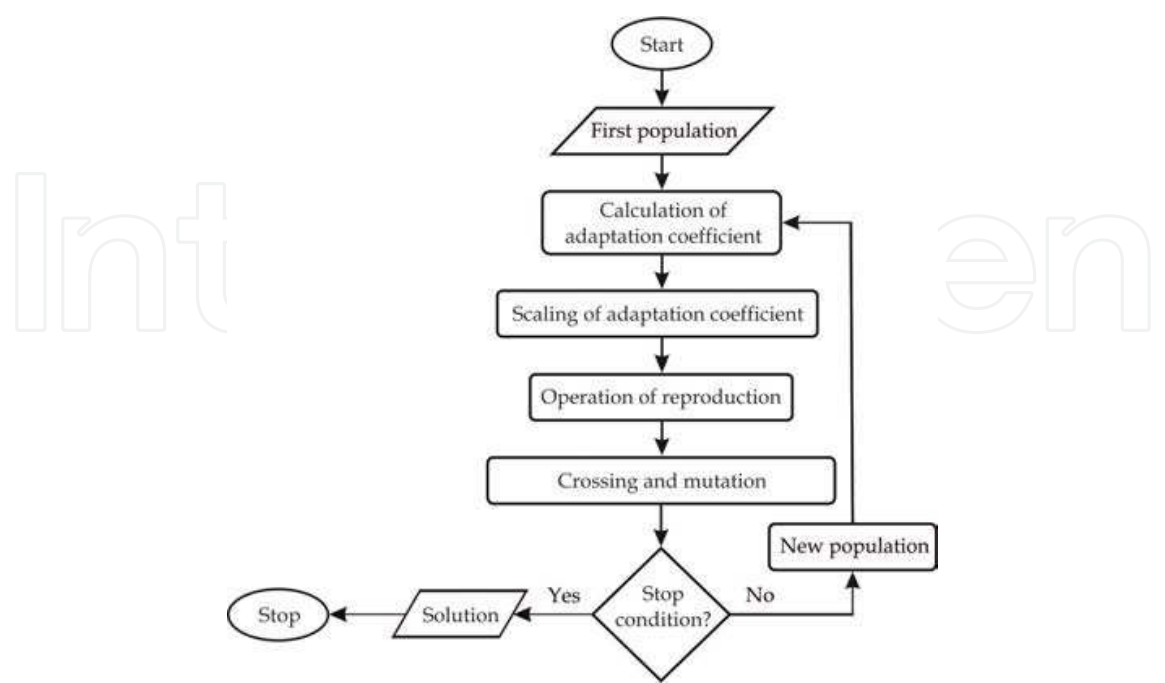Fig. 2. Flowchart of calibration procedure

Fig. 3. Flowchart of genetic algorithm

In order to form the next populations, it is necessary to determine the percentage share $\tilde{I}_c$ of each chromosome in I_N

$$
\begin{aligned}
\tilde{I}_{c_1} &= \frac{I_{c_1}}{I_N} 100\% \\
&\vdots \\
\tilde{I}_{c_n} &= \frac{I_{c_n}}{I_N} 100\%
\end{aligned}
\tag{20}
$$

Relations (19) and (20) allow for estimation of the usefulness of each chromosome in the population. The higher $\tilde{I}_c$ value of the given chromosome gives more probability to include it in the next population.

When the difference between the obtained values of adaptation coefficients is too small, it is necessary to carry out the scaling operation of the adaptation coefficient.

The next step is the operation of reproduction. According to the probability calculated by (20), the chromosomes from the initial population are selected at random. Depending on the value of $\tilde{I}_c$ coefficient, chromosomes have a bigger or smaller chance to be included in the next population. There are several ways of selection chromosomes for the new population. The most popular way is represented by the roulette wheel method. The results of random selection are rewritten to the new descendant population $(c_{21}, c_{22}, ..., c_{2n})$.

The next step is the crossing process. The chromosomes from the new population are joined in pairs in a random way and for the given crossing probability P_c are crossed or not.

The crossing is carried out according to the following formulae (Tomczyk, 2006):

The first crossing of paired d_{i1} and d_{j1} detectors gives

$$
\begin{aligned}
\tilde{d}_{i1} &= (1 - \alpha) d_{i1} + d_{j1} \\
\tilde{d}_{j1} &= \alpha\, d_{i1} + (1 - \alpha) d_{j1}
\end{aligned}
\tag{21}
$$

where: $\tilde{d}_{i1}$ is a descendant detector of i chromosome, and $\tilde{d}_{j1}$ is a descendant detector of j chromosome.

The coefficient α in (21) is selected according to

$$
\begin{aligned}
\alpha_{i\min} &= \frac{-d_{i1}}{d_{j1} - d_{i1}}, \quad \alpha_{i\max} = \frac{d_{i2} - d_{i1}}{d_{j1} - d_{i1}} \\
\alpha_{j\min} &= \frac{-d_{j1}}{d_{i1} - d_{j1}}, \quad \alpha_{j\max} = \frac{d_{j2} - d_{j1}}{d_{i1} - d_{j1}}
\end{aligned}
\tag{22}
$$

where: $\alpha_{i\min}$ and $\alpha_{i\max}$ present the minimum and maximum limit of α changeability for the detector from i chromosome, while $\alpha_{j\min}$ and $\alpha_{j\max}$ present minimum and maximum limit of α changeability for the detector from the j chromosome.

The changeability range of α is contained in the range between 0 and the third value calculated by means of (22) minus this value multiplied by Δ (sample interval of T).

Then the α value is selected at random from the above range, and is substituted into (21).

The second crossing of detectors d_{im} from i chromosome and d_{jm} from the j chromosome, where $k = 2, 3, ..., m$, gives

$$\begin{aligned}
\tilde{d}_{ik} &= (1-\alpha)d_{ik} + d_{jk} \\
\tilde{d}_{jk} &= \alpha\, d_{ik} + (1-\alpha)d_{jk}
\end{aligned} \tag{23}$$

where $\tilde{d}_{ik}$ is the k detector of i descendant chromosome and $\tilde{d}_{jk}$ is the k detector of j descendant chromosome.

Now, the coefficient α is selected according to

$$\begin{aligned}
\alpha_{i\min} &= \frac{d_{ik-1} - d_{ik}}{d_{jk} - d_{ik}}, \quad \alpha_{i\max} = \frac{d_{ik+1} - d_{ik}}{d_{jk} - d_{ik}} \\
\alpha_{j\min} &= \frac{d_{jk-1} - d_{jk}}{d_{ik} - d_{jk}}, \quad \alpha_{j\max} = \frac{d_{jk+1} - d_{jk}}{d_{ik} - d_{jk}}
\end{aligned} \tag{24}$$

For the i chromosome, the mutation operation is described by

$$\begin{aligned}
\tilde{d}_{ik} &= (\tilde{d}_{i(k+1)} - \tilde{d}_{i(k-1)})\,\alpha + \tilde{d}_{i(k-1)} \\
\alpha &\in [0,\,1], \quad k = 1, 2, ..., m
\end{aligned} \tag{25}$$

The time calculation of genetic algorithm can be reduced significantly if a stop condition is applied. It stops the calculation, if the value of $I_h(x)$ stored in memory does not change during a given number of iterations. (Tomczyk, 2006).

7. Algorithm for determining signals maximizing the absolute error

7.1 Signals constraint on magnitude

In the case of $D(x)$ error (15) the maximum $|y(t)|$ occurs for $t = T$

$$\max |y(t)| = y(T) = \int_0^T x(\tau) h(T - \tau)\, d\tau \tag{26}$$

if

$$x(\tau) = x_0(\tau) = \mathrm{a}\ sign[h(T - \tau)] \tag{27}$$

where a is the magnitude of $x(\tau)$.

Replacing τ by t in (26), we obtain

$$|y(t)| = y(T) = \int_0^T x(t) h(T - t)\, dt \tag{28}$$

and $x_0(t)$ maximizing (28) has now the form

$$x_0(t) = \text{a } sign[h(T - t)] \tag{29}$$

Substituting (29) into (28) gives

$$\max|y(t)| = y(T) = \text{a} \int_0^T |h(T - t)| dt = \text{a} \int_0^T |h(t)| dt \tag{30}$$

which can be computed in the very simple way.

7.2 Signals constraint on magnitude and rate of change

Let

$$x(t) = \int_0^t \phi(\tau) d\tau \tag{31}$$

then

$$y(T) = \int_0^T h(T - \tau) \int_0^t \phi(\tau) d\tau\, dt \tag{32}$$

Constraints related to $x(t)$ and $\upsilon(\tau)$ are as follows

$$| \int_0^t \phi(\tau) d\tau | = | x(t) | \le \text{a} \tag{33}$$

and

$$| \phi(t) | = | \dot{x}(t) | \le \vartheta \tag{34}$$

Changing the integration order in (32), we have

$$y(T) = \int_0^T \phi(\tau) \int_\tau^T h(T - t) dt\, d\tau \tag{35}$$

and after replacing τ for t, we get finally

$$y(T) = \int_0^T \phi(t) \int_t^T h(T - \tau) d\tau\, dt \tag{36}$$

A formula (36) proves that $\phi(t)$ maximizing $y(T)$ has the maximum magnitude $\phi(t) = \pm\vartheta$ by virtue of the formula (34) if

$$\phi(t) = sign \int_t^T h(T - \tau) d\tau \tag{37}$$

and $\phi(t) = 0$ in such subintervals, for which (33) between the switching moments has the form

$$|\int_0^t \phi(\tau)d\tau| > a \qquad (38)$$

Using the equations (32)-(38), we can determine signal $x_0(t)$ in the following cases

First case

When $|\int_0^t \upsilon_0(\tau)d\tau \neq \mathbf{a}|$ for ε varying in the intervals $[0,+\vartheta]$ and $[0,-\vartheta]$, (Fig. 4a,b), where

$\upsilon_0(t) = +\vartheta$ for $\int_t^T h(T-\tau)d\tau > +\varepsilon$ and $\upsilon_0(t) = -\vartheta$ for $\int_t^T h(T-\tau)d\tau < -\varepsilon$, than the signal $x_0(t)$ is

determined in three steps, according to Eqs. (39)-(47)..
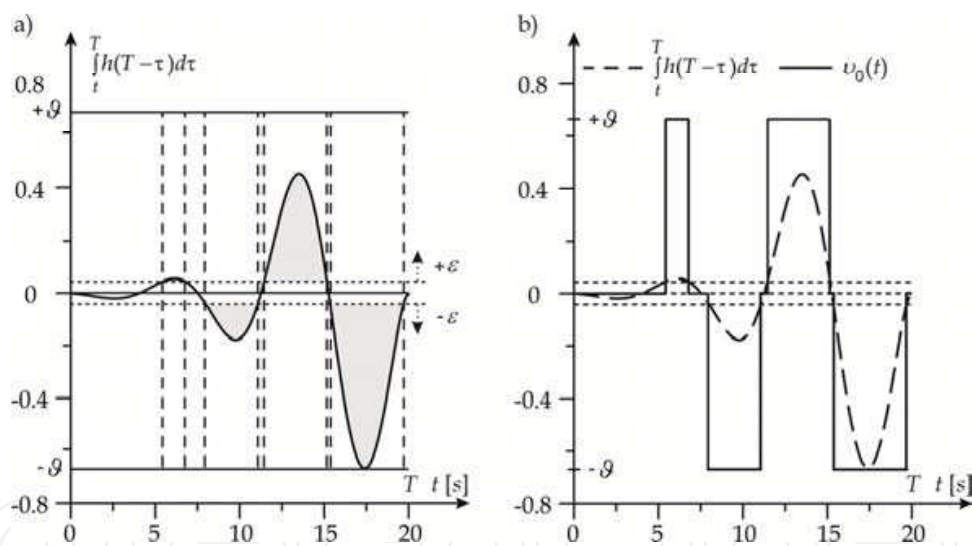
Fig. 4. Exemplary functions $\int_t^T h(T-\tau)d\tau$ and $\upsilon_0(t)$

During the first step, the 'bang-bang' functions $\upsilon_1(t)$ of the magnitude $\pm\vartheta$ are determined with switching moments resulting from (37) - Fig.5a

$$\begin{aligned} \upsilon_1(t) &= +\vartheta \quad \text{if } \phi(t) > 0 \\ \upsilon_1(t) &= -\vartheta \quad \text{if } \phi(t) < 0 \end{aligned} \qquad (39)$$

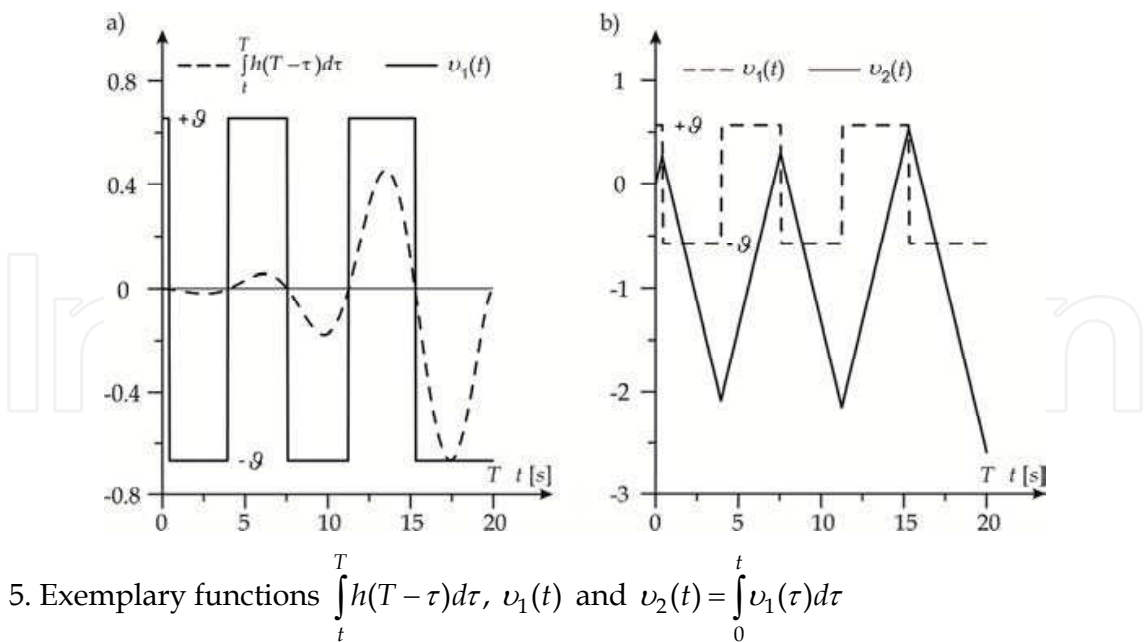In the second step, we obtain the function $\upsilon_2(t)$ by integrating $\upsilon_1(t)$ - Fig. 5b.

Fig. 5. Exemplary functions $\int\limits_t^T h(T-\tau)d\tau$, $\upsilon_1(t)$ and $\upsilon_2(t) = \int\limits_0^t \upsilon_1(\tau)d\tau$

Function $\upsilon_2(t)$ in particular switching intervals $t_1, t_2, ..., t_m$ of $\upsilon_1(t)$ is given by the following relations

for $t \le t_1$, $m = 1$

$$\upsilon_2(t) = \vartheta \cdot t \tag{40}$$

for $t_1 < t \le t_2$, $m = 2$

$$\upsilon_2(t) = \vartheta\, t_1 - \vartheta\, (t - t_1) \tag{41}$$

for $t_i < t \le t_{i+1}$, $i = 2, 3, ..., m$, $t_{m+1} = T$, m - number of switchings

$$\upsilon_2(t) = \vartheta\, t_1 + \vartheta \sum_{j=2}^{i} (-1)^{j-1} (t_j - t_{j-1}) + (-1)^i \vartheta\, (t - t_i) \tag{42}$$

In the last step, we determine the function $\upsilon_3(t)$ on the basis of $\upsilon_2(t)$:

$$\begin{aligned} \upsilon_3(t) &= \pm\vartheta & \text{if} \quad |\upsilon_2(t)| \le a \\ \upsilon_3(t) &= 0 & \text{if} \quad |\upsilon_2(t)| > a \end{aligned} \tag{43}$$

Finally, through integration of $\upsilon_3(t)$, we obtain the signal $x(t) = x_0(t)$ and this is the aim. This operation is shown in Fig. 6a.

During the intervals in which $\upsilon_3(t) = \pm\vartheta$, the signal shape is triangular, with the slope $\pm\vartheta$. In the intervals in which $\upsilon_3(t) = 0$, the signal is a constant and has the magnitude $\pm a$.

For m switching moments of $\upsilon_3(t)$ the value of error is described by the following equations:

for $m = 1$

$$y(T) = \frac{o_1}{t_1} \int_0^{t_1} h(T-\tau)\tau \, d\tau \; + \; \frac{o_T - o_1}{T - t_1} \int_{t_1}^T h(T-\tau)(\tau - t_1) \, d\tau \; + o_1 \int_{t_1}^T h(T-\tau) \, d\tau \tag{44}$$

for m ≥ 2

$$y(T) = \frac{o_1}{t_1} \int_0^{t_1} h(T-\tau)\tau \, d\tau + \sum_{i=2}^m \left[\frac{o_i - o_{i-1}}{t_i - t_{i-1}} \int_{t_{i-1}}^{t_i} h(T-\tau)(\tau - t_{i-1}) \, d\tau + o_{i-1} \int_{t_{i-1}}^{t_i} h(T-\tau) \, d\tau \right] +$$
$$+ \; \frac{o_T - o_m}{T - t_m} \int_{t_m}^T h(T-\tau)(\tau - t_m) \, d\tau + o_m \int_{t_m}^T h(T-\tau) \, d\tau \tag{45}$$

where $o_m = x_0(t_m)$, $o_T = x_0(T)$.

Fig. 6b presents the signal $x_0(t)$ and the error $y(t)$ corresponding to it
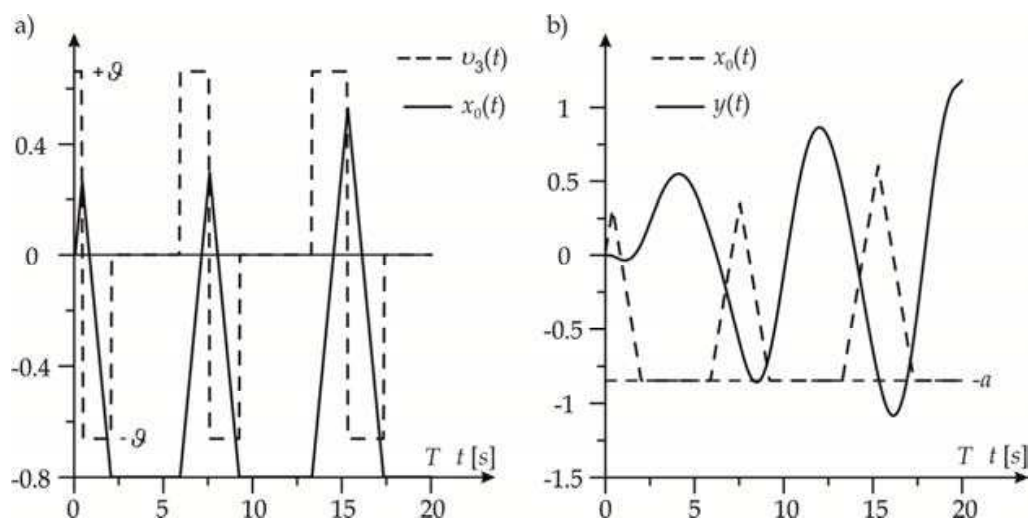
Fig. 6. Function $\upsilon_3(t)$, signal $x_0(t) = \int_0^t \upsilon_3(\tau) d\tau$ and error $y(t)$

The equations (44-45) in the discrete form are defined by:
for $n = 1$

$$y(N) = \frac{o_1}{t_1} \Delta \sum_{k=0}^{n_1} h(N-k)k + \frac{o_N - o_1}{N - n_1} \Delta \sum_{k=n_1}^{n_1} h(N-k)(k-n_1) + o_1 \Delta \sum_{k=n_1}^N h(N-k) \tag{46}$$

for $n \geq 2$

$$y(N) = \frac{o_1}{n_1} \Delta \sum_{k=0}^{n_1} h(N-k) \, k + \sum_{i=2}^m \left[\frac{o_i - o_{i-1}}{n_i - n_{i-1}} \Delta \sum_{k=n_{i-1}}^{n_1} h(N-k)(k-n_{i-1}) + o_{i-1} \Delta \sum_{k=n_{i-1}}^{n_1} h(N-k) \right]$$
$$+ \; \frac{o_N - o_m}{N - n_m} \Delta \sum_{k=n_m}^N h(N-k)(k-n_m) + o_m \Delta \sum_{k=n_m}^N h(N-k) \tag{47}$$

Second case

If $\vartheta \cdot T \leq a$ then the signal $x_0(t)$ is given directly by

$$x_0(t) = \vartheta \int_0^t sign[h(T - \tau)]d\tau \tag{48}$$

and the error equals

$$y(t) = \int_0^t x_0(\tau)h(t - \tau)d\tau \tag{49}$$

Equation (49) in the discrete form is defined by

$$y(N) = \sum_{k=0}^N x(k)h(n - k)\Delta, \text{ for } n = 0,1,...,N-1 \tag{50}$$

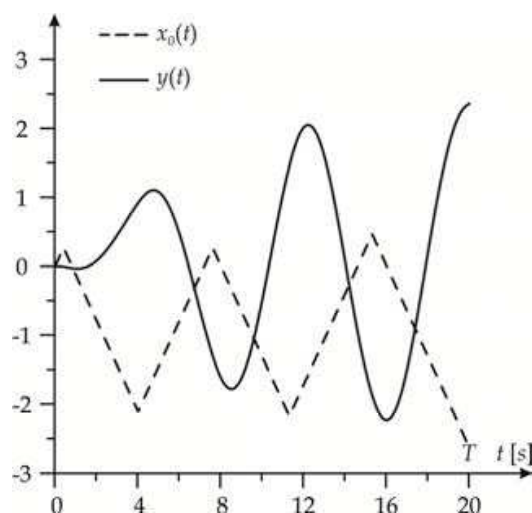Fig. 7 presents the signal $x_0(t)$ and error $y(t)$ obtained by (48)-(49)

Fig. 7. Signal $x_0(t)$ and error $y(t)$

Third case

If $\vartheta \cdot T > a$ then the signal $x_0(t)$ is determined indirectly by means of the functions $\upsilon_4(t)$ - $\upsilon_7(t)$

$$\upsilon_4(t) = \frac{\vartheta}{2a}\int_0^t h(T - \tau)(t - \tau)d\tau \tag{51}$$

$$\upsilon_5(t) = a \cdot sign[\upsilon_4(T - t)] \tag{52}$$

$$\upsilon_6(t) = \upsilon_5(t) \qquad \text{if } t \leq \frac{2a}{\vartheta}$$

$$\upsilon_6(t) = \upsilon_5(t) - \upsilon_5\left(t - \frac{2a}{\vartheta}\right) \quad \text{if } \frac{2a}{\vartheta} < t \leq T \tag{53}$$

$$\upsilon_7(t) = \upsilon_6(t)\frac{\vartheta}{a} \qquad \text{if} \quad t \le \frac{2a}{\vartheta}$$

$$\upsilon_7(t) = 0 \qquad \text{if} \quad \frac{a}{\vartheta} < t \le \frac{2a}{\vartheta} \qquad (54)$$

$$\upsilon_7(t) = \upsilon_6(t)\frac{\vartheta}{2a} \qquad \text{if} \quad \frac{2a}{\vartheta} < t \le T$$

Equation (51) in the discrete form is given by

$$\upsilon_4(n) = \frac{\vartheta}{2a}\Delta\sum_{k=0}^{n} h(n-k)(n-k), \quad n = 0, 1, \ldots, N-1 \qquad (55)$$

The functions $\upsilon_4(t)$ and $\upsilon_5(t)$ are shown in Fig. 8a, while $\upsilon_5(t)$ and $\upsilon_6(t)$ in Fig. 8b.
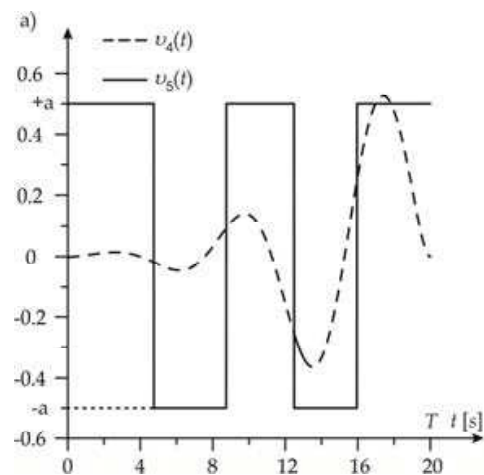
Fig. 8(a). Functions $\upsilon_4(t)$ and $\upsilon_5(t)$.   Fig. 8(b). Functions $\upsilon_5(t)$ and $\upsilon_6(t)$
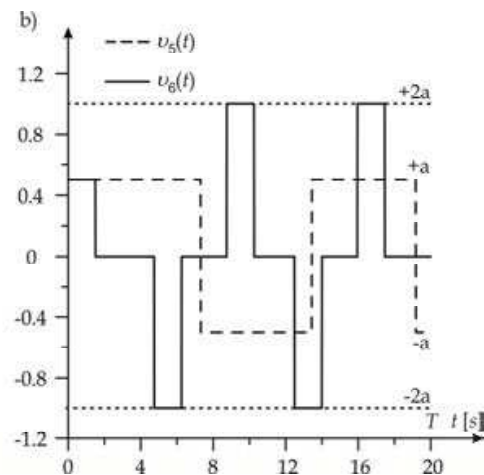
Fig. 9a presents the function $\upsilon_7(t)$ and the signal $x_0(t) = \int_0^t \upsilon_7(\tau)d\tau$, while the signal $x_0(t)$ and the error $y(t)$ corresponding to it are shown in Fig. 9b (Layer&Tomczyk, 2009; Layer&Tomczyk, 2010).
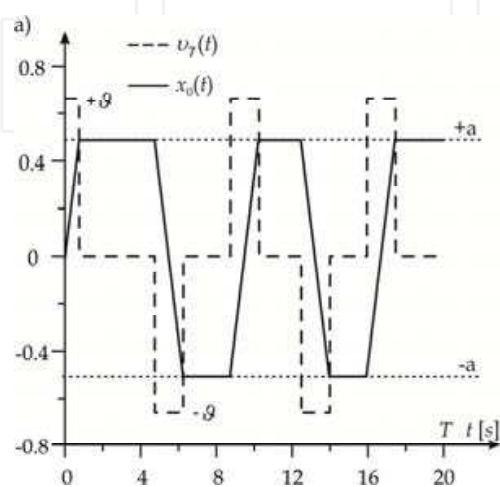

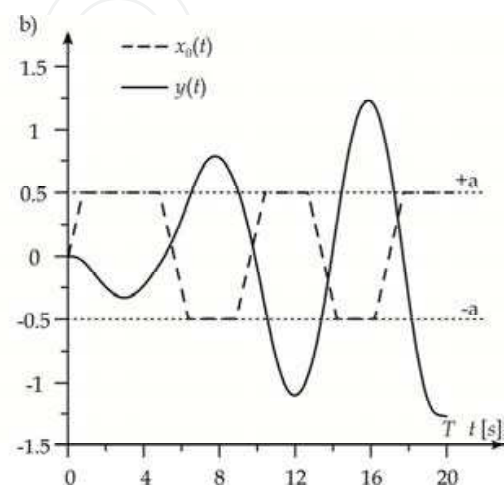Fig. 9(a). Function $\upsilon_7(t)$ and signal $x_0(t)$.   Fig. 9(b). Signal $x_0(t)$ and error $y(t)$

8. Maximum errors in optimization of models of measuring systems

In the technical domain the application of higher order models usually gives a possibility to better map the dynamic properties of real systems. On the other hand, the analysis of such models is most often difficult and time-consuming. Hence a tendency has developed to replace a higher order model by a simplified one. The class and order of such model are adopted in an arbitrary way. Its parameters can be determined by means of methods that minimize the mapping error, considering all possible input signals. Therefore it is suggested to solve the problem by using one signal which maximizes the error. In this way, the mapping error being determined is credible for any input. The application of the *minimax* method by means of the Levenberg-Marquardt algorithm (Tomczyk, 2009) gives good results.

This method includes two main numerical computation stages. At the first stage the $x_0(t)$ signal maximizing the error (Fig.10) is determined.
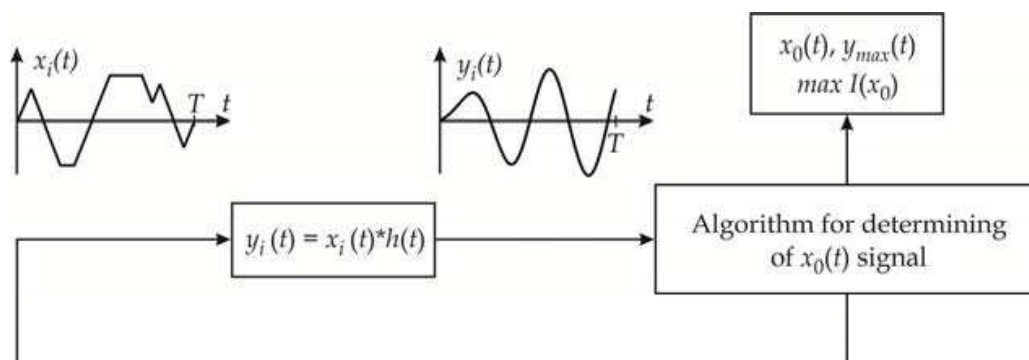

Fig. 10. Block diagram for determining $x_0(t)$ signal

At the second stage the class and order of the simplified model are adopted. For this model by means of $x_0(t)$ signal the parameters minimizing the error are determined.

The Levenberg-Marquardt algorithm is an iterative method, in which the vector of unknown parameters is determined in $k+1$ step by the following formula

$$\Xi_{k+1} = \Xi_k{}^T - \left[\mathbf{J}^T(\Xi_k, t)\mathbf{J}(\Xi_k, t) + \mu_k I \right]^{-1} \mathbf{J}^T(\Xi_k, t)y(\Xi_k, t) \tag{56}$$

with the error

$$I = \int_0^T y^2(\Xi_k, t)dt \tag{57}$$

where

$$y(\Xi_k, t) = \int_0^t h(t - \tau)x(\tau)\, d\tau \tag{58}$$

and

$$\mathbf{J}(\Xi_k,t) = \begin{bmatrix} \dfrac{\partial y(\Xi_k,t_1)}{\partial \xi_1} & \dfrac{\partial y(\Xi_k,t_1)}{\partial \xi_2} & \cdots & \dfrac{\partial y(\Xi_k,t_1)}{\partial \xi_m} \\[2mm] \dfrac{\partial y(\Xi_k,t_2)}{\partial \xi_1} & \dfrac{\partial y(\Xi_k,t_2)}{\partial \xi_2} & \cdots & \dfrac{\partial y(\Xi_k,t_2)}{\partial \xi_m} \\[2mm] \vdots & \vdots & \vdots & \vdots \\[2mm] \dfrac{\partial y(\Xi_k,t_n)}{\partial \xi_1} & \dfrac{\partial y(\Xi_k,t_n)}{\partial \xi_2} & \cdots & \dfrac{\partial y(\Xi_k,t_n)}{\partial \xi_m} \end{bmatrix} \tag{59}$$

The notations in (56)-(59) are as follows:

- $k = 1,2,...,p$, p - number of iteration loops
- $\mathbf{J}_{(n \times m)}(\Xi_k,t)$ - Jacobian matrix
- $\mathbf{I}_{(m \times m)}$ - unit matrix
- μ_k - scalar, its value changes during iteration
- $\Xi = [\xi_1,\xi_2,...,\xi_m]$ - model parameters searched for.

The Levenberg-Marquardt algorithm is used for computation in the following stages:

Stage 1, for $k=1$
1. Assume the initial values of the parameters of vector Ξ_k
2. Assume the initial value of the coefficient μ_k (e.g. μ_k = 0.1)
3. Solve the matrix equation (59) and calculate (58)
4. Calculate the value of error (57)
5. Determine the parameters of vector Ξ_{k+1}, following (56).

Stage 2 and further steps, for $k = 2,3,...,p$
1. Update the values of the parameters of vector Ξ_k
2. Solve the matrix equations (59), calculate (58) and (56)
3. Calculate the value of error (57)

Compare the values of error (57) for the step k and the step $k-1$. If the result is $y(\Xi_k,t) \geq y(\Xi_{k-1},t)$, multiply μ_k by the specified value $\lambda \in \Re$ (e.g. $\lambda = 10$) and return to the step 2 of stage 2. If the result is $y(\Xi_k,t) < y(\Xi_{k-1},t)$ divide μ_k by the value λ and return to the step 1 of stage 2.

Fig. 11. presents a block diagram of *minimax* optimization by means of the Levenberg-Marquardt algorithm.

The iteration process can be finished if in the consecutive stage the decrease in the value of error (57) is very small and insignificant. Then we fix $\mu_k = 0$ and determine the final result for the parameters of vector Ξ. If the coefficient μ_k is high, it means that the solution is not satisfactory, the values of the parameters of vector are not optimum and the value of error (57) is not at minimum level. At this point we can assumed

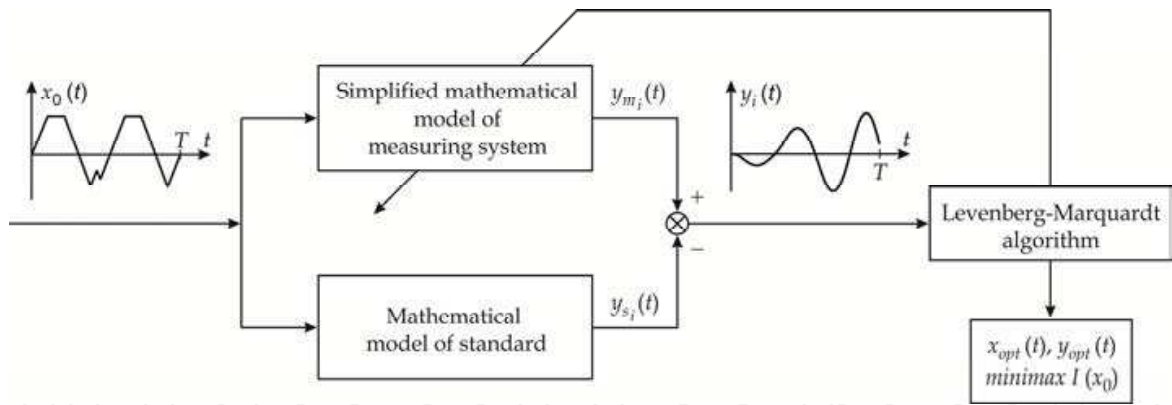$$\mathbf{J}^T(\Xi_k,t)\mathbf{J}(\Xi_k,t) << \mu_k\mathbf{I} \tag{60}$$

Fig. 11. Block diagram of *minimax* optimization by means of the Levenberg-Marquardt algorithm

In such a case the formula (60) leads to the steepest descent method

$$\Xi_{k+1} = \Xi_k{}^T - \frac{1}{\mu_k} \mathbf{J}^T(\Xi_k, t) y(\Xi_k, t) \tag{61}$$

If the value of coefficient μ_k is small, it means that the values of the parameters of vector Ξ are close to the optimum solution. Then

$$\mathbf{J}^T(\Xi_k, t) \mathbf{J}(\Xi_k, t) >> \mu_k \mathbf{I} \tag{62}$$

and the Levenberg-Marquardt algorithm is reduced to the Gauss-Newton method

$$\Xi_{k+1} = \Xi_k{}^T - \left[\mathbf{J}^T(\Xi_k, t) \mathbf{J}(\Xi_k, t) \right]^{-1} \mathbf{J}^T(\Xi_k, t) y(\Xi_k, t) \tag{63}$$

The selection of coefficient values μ_k and λ depends on the adopted programs and selected software.

9. Example of application

As an example let us consider the fourth order Butterworth, Tchebyhev and Bessel analog filters and integral-square error (14). These filters have the following transfer functions:

$$H_{Bt4}(s) = \frac{c}{\left[\left(\dfrac{s}{\omega_m} \right)^2 + 1.8478 \dfrac{s}{\omega_m} + 1 \right] \left[\left(\dfrac{s}{\omega_m} \right)^2 + 0.7654 \dfrac{s}{\omega_m} + 1 \right]} \tag{64}$$

$$H_{T4}(s) = \frac{c}{\left[5.5339 \left(\dfrac{s}{\omega_m} \right)^2 + 2.1853 \dfrac{s}{\omega_m} + 1 \right] \left[1.2039 \left(\dfrac{s}{\omega_m} \right)^2 + 0.1964 \dfrac{s}{\omega_m} + 1 \right]} \tag{65}$$

$$H_{Be4}(s) = \frac{c}{\left[0.4889 \left(\dfrac{s}{\omega_m} \right)^2 + 1.3397 \dfrac{s}{\omega_m} + 1 \right] \left[0.3890 \left(\dfrac{s}{\omega_m} \right)^2 + 0.7743 \dfrac{s}{\omega_m} + 1 \right]} \tag{66}$$

As a reference let us adopt the mathematical model of ideal low-pass filter given by (12) and (13) for $c = 1$ and $\omega_m = 100 \, \frac{rad}{s}$.

In order to determine the signals maximizing the error (14) let us adopt:

- magnitude $a = 0.2V$,

- rate of change , as a maximum absolute value of $\vartheta = \int_0^t h(\tau)d\tau$, where $h(t)$ is the difference between the impulse responses of filter and its standard: $\vartheta_{Bt4} = 1.11 \frac{V}{s}$, $\vartheta_{T4} = 1.36 \frac{V}{s}$ and $\vartheta_{Be4} = 1.01 \frac{V}{s}$ for Butterworth, Tchebyhev and Bessel filters respectively,

- $T = 0 - 0.5s.$,

- discretization step $\Delta = 0.001s$.

The obtained switching times of signals errors and their values for Butterworth, Tchebychev and Bessel filters are presented in Tables 1-3.

$T[s]$	Butterworth filter	
	$a = 0.2V$, $\vartheta = 1.11 \frac{V}{s}$	
	$x_0(t)$	$I(x_0)$
0	0	0
0.05	ϑ_+ [0.0, 0.045s.], ϑ_- [0.045, 0.05s.]	$8.67 \cdot 10^{-7}$
0.1	ϑ_+ [0.0, 0.095s.], ϑ_- [0.095, 0.1s.]	$4.57 \cdot 10^{-5}$
0.15	ϑ_+ [0.0, 0.13s.], ϑ_- [0.13, 0.15s.]	$2.68 \cdot 10^{-4}$
0.2	ϑ_+ [0.0, 0.185s.], $+a$ [0.185, 0.2s.]	$7.55 \cdot 10^{-4}$
0.25	ϑ_+ [0.0, 0.2s.], $+a$ [0.2, 0.25s.]	$19 \cdot 10^{-4}$
0.3	ϑ_+ [0.0, 0.185s.], $+a$ [0.185, 0.275s.], ϑ_- [0.275, 0.3s.]	$25 \cdot 10^{-4}$
0.35	ϑ_+ [0.0, 0.05s.], ϑ_- [0.05, 0.285s.], $-a$ [0.285, 0.35s.]	$39 \cdot 10^{-4}$
0.4	ϑ_+ [0.0, 0.08s.], ϑ_- [0.08, 0.345s.], $-a$ [0.345, 0.4s.]	$57 \cdot 10^{-4}$
0.45	ϑ_+ [0.0, 0.11s.], ϑ_- [0.11, 0.405s.], $-a$ [0.405, 0.45s.]	$79 \cdot 10^{-4}$
0.5	ϑ_+ [0.0, 0.135s.], ϑ_- [0.135, 0.455s.], $-a$ [0.455, 0.5s.]	$113 \cdot 10^{-4}$

Table 1. Time switchings and values of integral-square error for Butterworth filter

$T[s]$	Tchebychev filter	
	$a = 0.2,\ \vartheta = 1.36\dfrac{V}{s}$	
	$x_0(t)$	$I(x_0)$
0	0	0
0.05	ϑ_+ [0.0, 0.045s.], ϑ_- [0.045, 0.05s.]	$4.52 \cdot 10^{-6}$
0.1	ϑ_+ [0.0, 0.095s.], ϑ_- [0.095, 0.1s.]	$4.61 \cdot 10^{-5}$
0.15	ϑ_+ [0.0, 0.12s.], ϑ_- [0.12, 0.15s.]	$4.01 \cdot 10^{-4}$
0.2	ϑ_+ [0.0, 0.15s.], $+a$ [0.15, 0.2s.]	$12 \cdot 10^{-4}$
0.25	ϑ_+ [0.0, 0.15s.], $+a$ [0.15, 0.25s.]	$25 \cdot 10^{-4}$
0.3	ϑ_+ [0.0, 0.045s.], $+a$ [0.045, 0.24s.], ϑ_- [0.24, 0.3s.]	$36 \cdot 10^{-4}$
0.35	ϑ_+ [0.0, 0.07s.], ϑ_- [0.07, 0.29s.], $-a$ [0.29, 0.35s.]	$59 \cdot 10^{-4}$
0.4	ϑ_+ [0.0, 0.1s.], ϑ_- [0.1, 0.35s.], $-a$ [0.35, 0.4s.]	$87 \cdot 10^{-4}$
0.45	ϑ_+ [0.0, 0.125s.], ϑ_- [0.125, 0.4s.], $-a$ [0.4, 0.45s.]	$122 \cdot 10^{-4}$
0.5	ϑ_+ [0.0, 0.15s.], ϑ_- [0.15, 0.45s.], $-a$ [0.45, 0.5s.]	$173 \cdot 10^{-4}$

Table 2. Time switchings and values of integral-square error for Tchebychev filter

$T[s]$	Bessel filter	
	$a = 0.2,\ \vartheta = 1.01\dfrac{V}{s}$	
	$x_0(t)$	$I(x_0)$
0	0	0
0.05	ϑ_+ [0.0, 0.045s.], ϑ_- [0.045, 0.05s.]	$8.55 \cdot 10^{-8}$
0.1	ϑ_+ [0.0, 0.095s.], ϑ_- [0.095, 0.1s.]	$5.66 \cdot 10^{-5}$
0.15	ϑ_+ [0.0, 0.12s.], ϑ_- [0.12, 0.15s.]	$2.74 \cdot 10^{-4}$
0.2	ϑ_+ [0.0, 0.15s.], $+a$ [0.15, 0.2s.]	$7.28 \cdot 10^{-4}$
0.25	ϑ_+ [0.0, 0.15s.], $+a$ [0.15, 0.25s.]	$18 \cdot 10^{-4}$
0.3	ϑ_+ [0.0, 0.045s.], $+a$ [0.045, 0.24s.], ϑ_- [0.24, 0.3s.]	$25 \cdot 10^{-4}$
0.35	ϑ_+ [0.0, 0.07s.], ϑ_- [0.07, 0.29s.], $-a$ [0.29, 0.35s.]	$37 \cdot 10^{-4}$
0.4	ϑ_+ [0.0, 0.1s.], ϑ_- [0.1, 0.35s.], $-a$ [0.35, 0.4s.]	$51 \cdot 10^{-4}$
0.45	ϑ_+ [0.0, 0.125s.], ϑ_- [0.125, 0.4s.], $-a$ [0.4, 0.45s.]	$70 \cdot 10^{-4}$
0.5	ϑ_+ [0.0, 0.15s.], ϑ_- [0.15, 0.45s.], $-a$ [0.45, 0.5s.]	$99 \cdot 10^{-4}$

Table 3. Time switchings and values of integral-square error for Bessel filter

Fig. 12 presents signals $x_0(t)$ and errors $y(t)$ as well as Fig. 13 illustrates the integral-square error as function of time duration $T = 0-0.5\ s.$ for $\Delta T = 0.05s.$
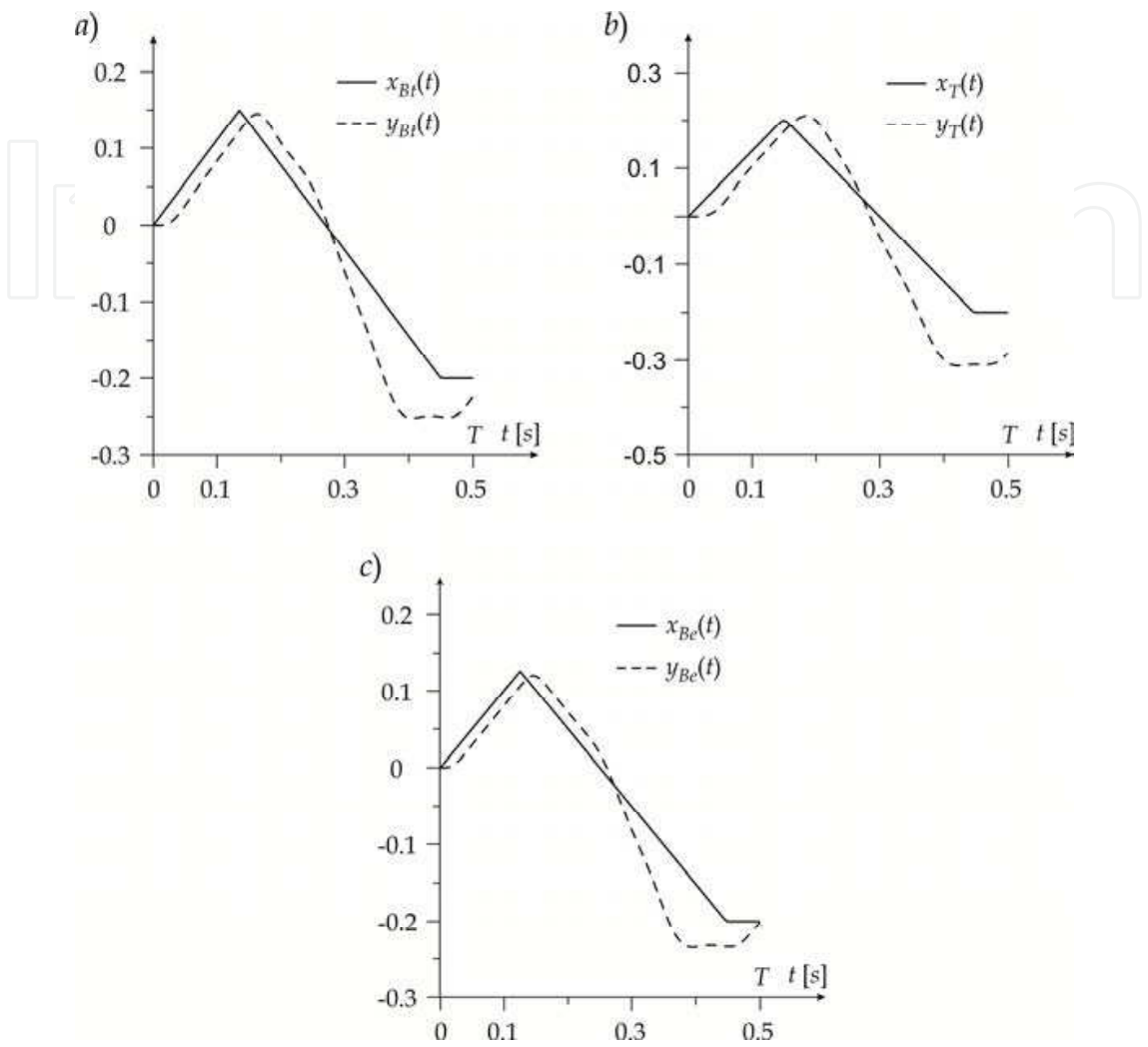

Fig. 12. Signals $x_0(t)$ and error $y(t)$ for Butterworth a), Tchebyhev b) and Bessel c) filters.
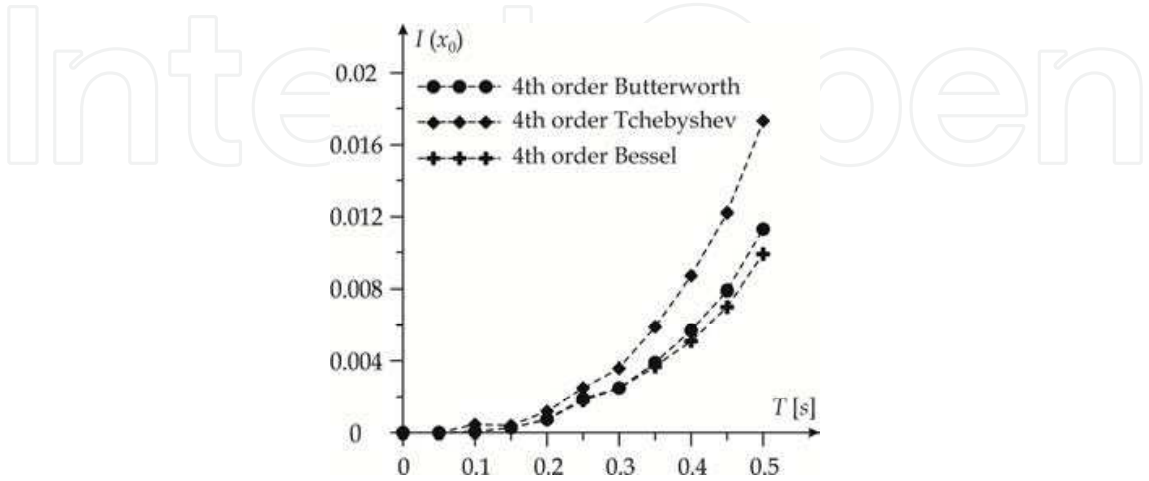

Fig. 13. Integral-square error as function of time duration $T = 0-0.5\ s.$ for Butterworth, Tchebychev and Bessel filters.

From Fig. 13 it follows that for $T < 0.2\,s$. signal $x_0(t)$ generates similar values of error for all filters. In the interval $0.2\,s. < T < 0.35\,s$. the highest value of error generates the Tchebyshev filter, however for the Butterworth and Bessel filters the values of error are similar. For $T > 0.35\,s$. the higher error generates the Tchebyshev filter, whereas the Bessel filter generates the lowest value.

10. Conclusion

The calibration of systems based on the theory of maximum dynamic errors, makes it possible to create accuracy classes for such dynamic systems and the hierarchy of dynamic accuracy resulting from them. These hierarchies are valid regardless of the shape of the measured dynamic signal that can appear at the input of the investigated system.

The calibration methods presented in this chapter can be widely applied in many different domains, eg. in electrical metrology (transducers, strain gauge amplifiers, filters, etc), geophysics (accelerometer and vibrometer systems), medicine (electroencephalograph and electrocardiograph systems), meteorology (autocomparators, autobridges), etc.

11. References

Layer, E. (2002). *Modelling of Simplified Dynamical Systems,* Springer-Verlag, ISBN 3-540-43762-2, Berlin Heidelberg

Layer, E.; Tomczyk, K. (2009). *Determination of non-standard input signal maximizing the absolute error*, Metrology and Measurement Systems. Vol. XVII, no. 2, pp. 199-208, ISSN 0860-8229

Layer, E.; Tomczyk, K. (2010). *Measurements, Modelling and Simulation of Dynamic Systems*, Springer-Verlag, ISBN 978-3-642-04587-5, Berlin Heidelberg

Tomczyk, K. (2006). *Application of genetic algorithm to measurement system calibration intended for dynamic measurement*, Metrology and Measurement Systems. Vol. XIII, no. 1, pp. 93-103, ISSN 0860-8229

Tomczyk, K. (2009). Levenberg-Marquardt Algorithm for Optimization of Mathematical Models according to Minimax Objective Function of Measurement Systems, Metrology and Measurement Systems. Vol. XVI, no. 4, pp. 599-606, ISSN 0860-8229

Tomczyk, K. (2011). *Procedure for correction of the ECG signal error introduced by skin-electrode interface*, Metrology and Measurement Systems. Vol. XVIII, no. 3, pp. 461-470, ISSN 0860-8229

Tomczyk, K.; Sieja, M. (2006). *Acceleration transducers calibration based on maximum dynamic error*, Czasopismo Techniczne 3-E, Cracow University of Technology, pp. 37-49, ISSN 0011-4561
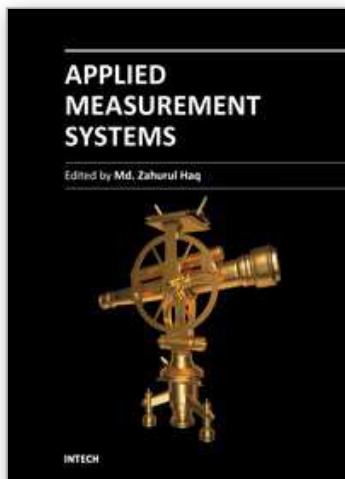
Applied Measurement Systems

Edited by Prof. Zahurul Haq

ISBN 978-953-51-0103-1

Hard cover, 390 pages

Publisher InTech

Published online 24, February, 2012

Published in print edition February, 2012

Measurement is a multidisciplinary experimental science. Measurement systems synergistically blend science, engineering and statistical methods to provide fundamental data for research, design and development, control of processes and operations, and facilitate safe and economic performance of systems. In recent years, measuring techniques have expanded rapidly and gained maturity, through extensive research activities and hardware advancements. With individual chapters authored by eminent professionals in their respective topics, Applied Measurement Systems attempts to provide a comprehensive presentation and in-depth guidance on some of the key applied and advanced topics in measurements for scientists, engineers and educators.

How to reference

In order to correctly reference this scholarly work, feel free to copy and paste the following:

Krzysztof Tomczyk (2012). Calibration of Measuring Systems Based on Maximum Dynamic Error, Applied Measurement Systems, Prof. Zahurul Haq (Ed.), ISBN: 978-953-51-0103-1, InTech, Available from: http://www.intechopen.com/books/applied-measurement-systems/calibration-of-measuring-systems-based-on-maximum-dynamic-error

INTECH
open science | open minds